

Optimized Spectrum-Shaping Strategy for Coded Single-Carrier Transmission

Xiaojun Yuan, Haitao Li, Li Ping, *Senior Member, IEEE*, and Xiaokang Lin

Abstract—We investigate spectrum shaping based on cyclic filtering for coded single-carrier transmission over intersymbol interference (ISI) channels. An optimized precoder is derived for coded single-carrier systems using an iterative linear-minimum-mean-square-error (LMMSE) frequency-domain-equalization (FDE) receiver. Numerical results show that this precoder can provide considerable spectrum-shaping gain.

Index Terms—Intersymbol interference (ISI) channels, iterative linear-minimum-mean-square-error frequency-domain-equalization (LMMSE-FDE), signal-to-noise-ratio (SNR) -variance evolution, spectrum shaping.

I. INTRODUCTION

INFORMATION theory shows that shaping the input spectrum of an intersymbol interference (ISI) channel can potentially improve system performance. The optimum spectrum that maximizes channel mutual information is the well-known water-filling solution [1]. Orthogonal frequency-division multiplexing (OFDM) provides a straightforward means for spectrum shaping. However, multiple codes with different rates are required in this approach, which incurs high complexity at both the transmitter and receiver sides. Recently, it is shown that spectrum shaping can be realized in single-carrier systems using a cyclic-filtering precoder [2]. The precoder in [2] aims to maximize the output signal-to-noise-ratio (SNR) of linear-minimum-mean-square-error (LMMSE) frequency-domain-equalization (FDE). Its advantage over water-filling was demonstrated in [2] for systems with non-iterative equalization and decoding.

This letter focuses on the realization of spectrum-shaping gain using a single code for a receiver involving iterative LMMSE equalization and decoding. We show that the strategy in [2] can be viewed as to maximize the output SNR of the iterative LMMSE equalizer at the first iteration, which is not optimal for the overall iterative process. We formulate the precoder optimization problem based on the SNR-variance evaluation technique developed in [3], and we prove the convexity of this

problem. This allows us to find the optimum solution using standard optimization tools. Numerical results demonstrate that the proposed precoder can considerably outperform the precoder in [2] as well as the water-filling precoder.

The focus of this letter is spectrum shaping instead of suppressing the ISI effect. This distinguishes our work from some other existing precoding approaches, such as [4] and [5].

The main advantage of the proposed scheme, compared to OFDM, is the achievement of spectrum-shaping gain with a single code, which avoids the complexity of implementing multiple codes. On the other hand, similar to OFDM and other precoding schemes [4], [5], the proposed precoder results in a high peak-to-average-power ratio (PAPR). Interestingly, the proposed scheme is more flexible in this respect, since the transmitter can simply turn off precoding so as to reduce PAPR (but then it cannot enjoy spectrum-shaping gain either). For OFDM, however, high PAPR is always a problem with or without spectrum shaping.

II. SIGNALING MODEL

Consider the transmission with cyclic-prefix (CP) [6] insertion over a quasi-static complex-valued ISI channel. The received signal vector \mathbf{r} can be expressed as

$$\mathbf{r} = \mathbf{h} \otimes \mathbf{y} + \boldsymbol{\eta} \quad (1)$$

where \mathbf{y} is the transmitted signal vector of block length J (not including CP), \mathbf{h} the time-domain ISI channel vector with L taps, “ \otimes ” the circular convolution operator, $\boldsymbol{\eta} \sim \mathcal{CN}(\mathbf{0}, \sigma^2 \mathbf{I})$ the additive noise, and \mathbf{I} an identity matrix with a proper size. Throughout this letter, we assume perfect channel state information (CSI) at both the transmitter and receiver sides.

The transmitted signal is generated as follows:

$$\mathbf{y} = \mathbf{a} \otimes \mathbf{x} \quad (2)$$

where \mathbf{a} is a precoding vector, and \mathbf{x} is a coded vector. Then, (1) can be rewritten as

$$\mathbf{r} = \mathbf{h} \otimes (\mathbf{a} \otimes \mathbf{x}) + \boldsymbol{\eta} = \mathbf{h}^* \otimes \mathbf{x} + \boldsymbol{\eta} \quad (3)$$

where the joint effect of the precoder and the physical channel forms a composite ISI channel characterized by

$$\mathbf{h}^* \equiv \mathbf{h} \otimes \mathbf{a}. \quad (4)$$

Manuscript received May 31, 2008; revised August 29, 2008. This work was supported by a grant from the Research Grant Council of the Hong Kong SAR, China [Project No. CityU 117007]. This material is presented in part at the 5th International Symposium Turbo Codes & Related Topics, Lausanne, Switzerland, September 2008. The associate editor coordinating the review of this manuscript and approving it for publication was Prof. Yimin Zhang.

X. Yuan and L. Ping are with the Department of Electronic Engineering, City University of Hong Kong, Kowloon, Hong Kong (e-mail: xjyuan@cityu.edu.hk; eeliping@cityu.edu.hk).

H. Li and X. Lin are with the Department of Electronic Engineering, Tsinghua University, Beijing 100084, China (e-mail: lht02@mails.tsinghua.edu.cn; linxk@sz.tsinghua.edu.cn).

Digital Object Identifier 10.1109/LSP.2008.2006712

Let \mathbf{A} (resp., \mathbf{X}) be the discrete Fourier transform (DFT) of \mathbf{a} (resp., \mathbf{x}). Then, (2) can be expressed as

$$\mathbf{y} = \text{IDFT}(\mathbf{A} \odot \mathbf{X}) \quad (5)$$

where $\text{IDFT}(\cdot)$ represents the inverse DFT operation, and “ \odot ” denotes entry-wise multiplication. The complexity involved in (5) is $O(J \log J)$ using fast Fourier transform (FFT). The implementation of the above precoding scheme is illustrated in the upper part of Fig. 1. From (5), we can readily shape the spectrum of the channel input \mathbf{y} by adjusting \mathbf{A} .

III. ITERATIVE LMMSE-FDE AND PRECODER OPTIMIZATION

A. Iterative LMMSE-FDE Receiver

Assume that the encoder in Fig. 1 generates a coded random sequence \mathbf{x} with

$$\text{Cov}(\mathbf{x}, \mathbf{x}) = \text{Cov}(\mathbf{X}, \mathbf{X}) = \mathbf{I} \quad (6)$$

which can be approximately ensured using random interleaving. Iterative joint equalization and decoding can then be applied at the receiver to efficiently cancel ISI.

A standard iterative receiver [3], [8] is shown in the lower part of Fig. 1. The receiver refines the estimate of \mathbf{x} by iteratively executing two modules, namely, the elementary signal estimator (ESE) that handles the effect of the composite channel \mathbf{h}^* and the decoder (DEC) that performs the standard *a posteriori* probability (APP) decoding based on the soft message from the ESE. The ESE considered in this letter follows the LMMSE-FDE principle developed in [3]. The complexity involved is independent of the number of channel taps [3], and so it remains the same with and without the precoder.

B. SNR-Variance Evolution

Analysis in [3] shows that the behavior of an iterative LMMSE-FDE receiver can be conveniently characterized by a variable pair ρ and v , where ρ represents the output SNR of the ESE (also the input SNR of the DEC), and v represents the input variance of the ESE (also the output variance of the DEC). The SNR-variance transfer functions of the ESE and the DEC are denoted, respectively, by $\rho = \phi(v)$ and $v = \psi(\rho)$. The evolution process then reduces to a recursion of ρ and v . More specifically, v is initialized to 1 based on (6) (implying no *a priori* information on \mathbf{x} is available). The evolution process continues when

$$\phi(v) > \psi^{-1}(v) \quad (7)$$

and converges to a fixed point (v_0, ρ_0) with

$$\phi(v_0) = \psi^{-1}(v_0). \quad (8)$$

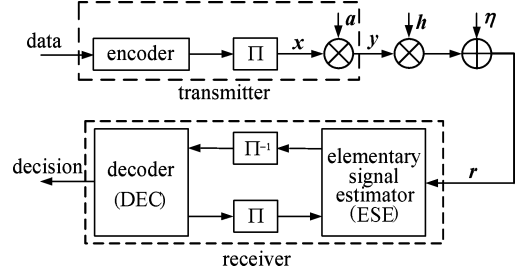


Fig. 1. Diagram of the proposed transceiver. Π represents the random interleaver, and Π^{-1} represents the corresponding de-interleaver.

At this point, the BER performance of the system can be estimated using a pre-simulated function $\text{BER} = g(v_0)$.

It is shown in [3] that the transfer function ϕ of the ESE can be expressed as

$$\phi(v) = \left(\frac{1}{J} \sum_{j=0}^{J-1} \left(v^{-1} + \frac{|g_j^*|^2}{\sigma^2} \right)^{-1} \right)^{-1} - v^{-1} \quad (9)$$

where g_j^* is the spectrum of \mathbf{h}^* at the j th frequency point that satisfying

$$g_j^* = g_j A_j \quad (10)$$

with g_j and A_j being the j th entry of the DFT of \mathbf{h} and \mathbf{a} , respectively. In practice, $\psi(\cdot)$ and $g(\cdot)$ are generated by pre-simulating the DEC in AWGN channels.

C. Precoder Optimization

From (9), the behavior of the ESE depends on the spectrum coefficients $\{g_j^*\}$ of the composite channel, and so on those of the precoder [cf., (10)]. We can thus tune the system performance by properly selecting \mathbf{A} . The optimization objective and constraints are summarized as follows.

- We want to minimize the transmission power $\sum_{j=0}^{J-1} |A_j|^2$ measured at \mathbf{y} (see Fig. 1).
- We need to ensure that the iterative receiver converges to a designated output variance v_0 , where v_0 is determined by the target $\text{BER} = g(v_0)$ of the system.

Let $w_j \equiv |A_j|^2$ for $\forall j$. The precoder optimization problem can be formulated as

$$\min_{\{w_j \geq 0\}} \sum_{j=0}^{J-1} w_j \quad (11a)$$

$$\text{s.t. } \phi(v) > \psi^{-1}(v), \text{ for } 1 \geq v > v_0. \quad (11b)$$

The following proposition is useful in solving (11).

Proposition 1: ϕ in (9) is concave in $\{w_j\}$.

Proof: Let

$$q_j \equiv v^{-1} + |g_j^*|^2/\sigma^2 = v^{-1} + w_j|g_j|^2/\sigma^2$$

for $j = 0, 1, \dots, J-1$. We then only need to show that

$$\phi(\{q_j\}) = J \cdot \left(\sum_{j=0}^{J-1} q_j^{-1} \right)^{-1} - v^{-1} \quad (12)$$

is concave in $\{q_j\}$ for $q_j > 0, \forall j$. A family of well-defined functions is given as follows:

$$p_j(z, q_j) = (z^{-1} + q_j^{-1})^{-1}, \text{ for } j = 0, 1, \dots, J-1.$$

It is straightforward to verify that the Hessian matrix

$$\begin{bmatrix} \frac{\partial^2 p_j}{\partial z^2} & \frac{\partial^2 p_j}{\partial q_j \partial z} \\ \frac{\partial^2 p_j}{\partial z \partial q_j} & \frac{\partial^2 p_j}{\partial q_j^2} \end{bmatrix} = -\frac{2}{(z + q_j)^3} \begin{bmatrix} -q_j \\ z \end{bmatrix} \begin{bmatrix} -q_j & z \end{bmatrix} \quad (13)$$

is semi-negative definite for $z > 0$ and $q_j > 0$. Thus, $p_j(z, q_j)$ is concave in $\{z, q_j\}$. Together with the fact that $p_j(z, q_j)$ is non-decreasing in both z and q_j , $p_{j+1} \circ p_j \equiv p_{j+1}(p_j(z, q_j), q_{j+1})$ is concave in $\{z, q_j, q_{j+1}\}$ [7]. Applying this notion recursively for $j = 1, 2, \dots, J-2$ and then letting $z = q_0$, we obtain that

$$p_{J-1} \circ p_{J-2} \circ \dots \circ p_1 = \left(\sum_{j=0}^{J-1} q_j^{-1} \right)^{-1} \quad (14)$$

is concave in $\{q_j\}$ and so is $\phi(\{q_j\})$, which concludes the proof.

We can then solve (11) as follows. We require that the constraint $\phi(v) > \psi^{-1}(v)$ holds on the discrete points of v in $(v_0, 1]$ in finding the minimum transmission power. With Proposition 1, these constraints are convex, and so the problem can be solved using standard convex optimization tools [7]. For a large J , directly solving (11) can be time-consuming. To overcome this problem, we can solve (11) for an auxiliary system with a shorter block length $J' < J$ over the same channel defined by \mathbf{h} in (1). In this way, we obtain an optimized precoder spectrum \mathbf{A}' (with the time-domain precoding sequence denoted by \mathbf{a}') for the auxiliary system. We then approximate the desired time-domain precoding sequence \mathbf{a} by padding \mathbf{a}' with zeros, or equivalently speaking, we approximate \mathbf{A} by interpolating \mathbf{A}' (i.e., over-sampling in the frequency domain). The performance loss related to this approximate method is usually marginal, as verified by the numerical results provided later.

TABLE I
MINIMUM SNR VERSUS J' IN THE PROAKIS B
CHANNEL. TARGET BER = 10^{-5}

J'	4	8	16	32	64	$\approx +\infty$
SNR (dB)	1.876	1.748	1.745	1.743	1.741	1.741

IV. NUMERICAL RESULTS AND DISCUSSIONS

To evaluate the system performance, we define the SNR as the ratio of the transmission signal power over the channel noise power, i.e.,

$$\text{SNR} \equiv \frac{\mathbb{E}[\|\mathbf{y}\|^2]}{\mathbb{E}[\|\boldsymbol{\eta}\|^2]} = \frac{\sum_{j=0}^{J-1} w_j}{J \cdot \sigma^2} \quad (15)$$

where $\|\cdot\|$ represents the Euclidean distance. Note that minimizing SNR in (15) is equivalent to minimizing $\sum_{j=0}^{J-1} w_j$.

We will use two alternatives, namely, the water-filling precoder and the one proposed in [2],¹ for comparison. The water-filling precoder is based on the well-known water-filling principle [1] for parallel channels. We can first find such a water-filling solution in the frequency domain and then obtain the time-domain precoding sequences [i.e., \mathbf{a} in (2)] using DFT. The precoder derived in [2] is for non-iterative LMMSE equalization (that can be seen as a special case of the proposed scheme terminated at the first iteration).

We first demonstrate the performance of the optimized precoder in the Proakis B channel [9] (with coefficients [0.407 0.815 0.407]). The ENC in Fig. 1 is realized by a rate-1/2 convolutional code with generation polynomials $(23, 35)_8$ followed by random interleaving and quadrature-phase-shift-keying (QPSK) modulation. The information bit length is 32 768. Table I lists the minimum SNR obtained by solving (11) at different J' for the auxiliary systems (see the related discussions at the end of the last section). From Table I, we can see that the minimum SNR is close to the ultimate limit for a moderate J' (say, $\geq 10L$).

The BER performance of the systems with the optimized precoder, the water-filling precoder, the precoder in [2], and no precoder, respectively, is illustrated in Fig. 2. $J' = 64$ and iteration number = 30. The performance predicted by evolution and the water-filling capacity of the channel at rate $R = 1$ bit/symbol are also marked for reference. We can see that the performance of the optimized precoder depends on its target BER. Particularly, at BER = 10^{-5} , the optimized precoder with target BER = 10^{-5} outperforms the un-precoded system by 2.9 dB. It also outperforms the water-filling precoder by 0.4 dB and the precoder in [2] by 1.5 dB, respectively. This shows the advantage of the optimized precoder.

We next demonstrate the precoder performance in a three-tap Rayleigh block-fading ISI channel. The average channel power is normalized to 1, i.e., $\mathbb{E}[\|\mathbf{h}\|^2] = 1$. The settings remain the same as those in Fig. 2, except that the block length = 8192 and iteration number = 15. The precoder is optimized for each transmission block with target BER = 10^{-3} .

¹It can be shown that the precoder proposed in [2] is the solution to maximizing ϕ in (9) at $v = 1$. This is the initial output SNR of the ESE when it terminates at the first iteration (i.e., a non-iterative receiver).

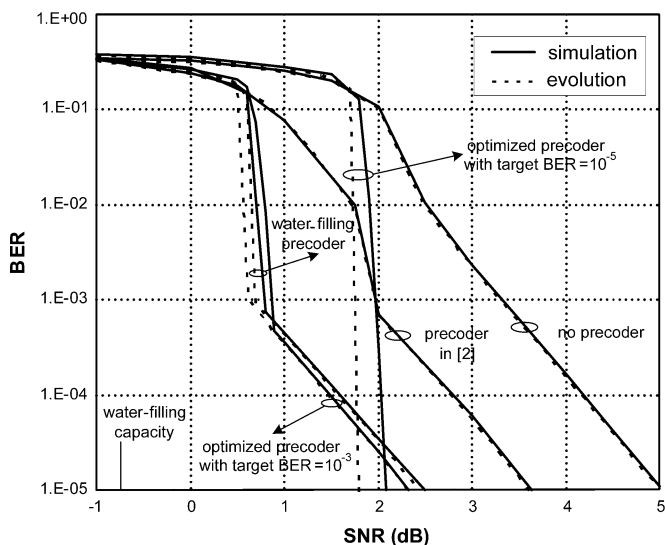


Fig. 2. BER performance of the systems with the optimized precoder, the water-filling precoder, the precoder in [2], and no precoder, respectively, over the Proakis B channel.

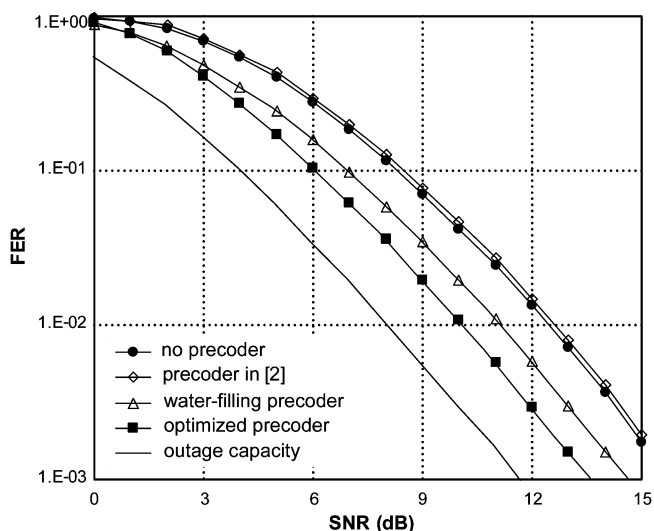


Fig. 3. FER performance of the systems in Fig. 2 over the 3-tap Rayleigh fading ISI channel.

Fig. 3 compares the frame-error-rate (FER) performance of the various precoders. The channel outage capacity at $R = 1$ bit/symbol is also included for reference. We can see that the optimized precoder achieves 2.2 dB gain compared with the non-precoded system. It also outperforms the water-filling precoder by 1.0 dB. Note that the use of the precoder in [2] in this case worsens the system performance by 0.1 dB. This implies that the precoder in [2] (that maximizes the output SNR of the ESE for the first iteration) can have negative effect to systems involving iterative joint equalization and decoding.

Also note that every curve in Fig. 3 is obtained by setting the total power of each transmitted block to a constant (including the one for computing outage capacity) and changing the distribution of the power among sub-carriers. The total transmission power does not vary from block to block, even though the

total channel gain does vary from block to block. This is because the “no precoder” system (that serves as reference) assumes no feedback CSI at the transmitter, and so it is unable to adjust the total transmission power according to the channel condition. To make a fair comparison, all of the other curves follow the same equal-power constraint, although the systems with precoding are actually able to adjust their total power levels (in addition to spectrum shaping) based on the feedback CSI. Such adjustment may bring about considerable performance gain, but such gain does not fall in the interest of this letter.

It is shown in Figs. 2 and 3 that there is a relatively large gap between the simulated performance and the channel capacity. Reducing this gap by joint optimization of the precoder and the channel codes is an interesting future research topic.

V. CONCLUSION

In this letter, a precoding method is proposed for single-carrier transmission over ISI channels. It consists of the following ingredients.

- Only one code is involved, which avoids the difficulties in implementing multiple codes in OFDM.
- The precoder can be efficiently implemented using FFT. The convolution effect of the precoder does not incur extra cost in the LMMSE-FDE at the receiver.
- The precoder can be optimized based on the SNR-variance evolution. Noticeable performance improvement is observed.
- In the proposed scheme, the transmitter has the freedom to turn off precoding to avoid high PAPR or to turn on it to achieve spectrum-shaping gain.² This is more flexible than OFDM for which high PAPR is always a problem with or without spectrum shaping.

REFERENCES

- [1] T. M. Cover and J. A. Thomas, *Elements of Information Theory*. New York: Wiley, 1991.
- [2] D. Z. Filho, L. Féty, and M. Terré, “A hybrid single carrier multicarrier scheme with power allocation,” *EURASIP J. Wireless Commun. Network.*, vol. 2008, p. 11, ID168032.
- [3] X. Yuan, Q. Guo, X. Wang, and L. Ping, “Evolution analysis of low-cost iterative equalization in coded linear systems with cyclic prefixes,” *IEEE J. Select. Areas Commun.*, vol. 26, no. 2, pp. 301–310, Feb. 2008.
- [4] M. Tomlinson, “New automatic equalizer employing modulo arithmetic,” *Electron. Lett.*, vol. 7, no. 5, pp. 138–139, Mar. 1971.
- [5] K. Takeda, H. Tomeba, and F. Adachi, “Joint Tomlinson-Harashima precoding and frequency-domain equalization for broadband single-carrier transmission,” *IEICE Trans. Commun.*, vol. E91-B, no. 1, pp. 258–266, Jan. 2008.
- [6] D. Tse and P. Viswanath, *Fundamentals of Wireless Communication*. Cambridge, U.K.: Cambridge Univ. Press, 2005.
- [7] S. Boyd and L. Vandenberghe, *Convex Optimization*. Cambridge, U.K.: Cambridge Univ. Press, 2004.
- [8] M. Tüchler, R. Koetter, and A. Singer, “Turbo equalization: Principles and new results,” *IEEE Trans. Commun.*, vol. 50, no. 5, pp. 754–767, May 2002.
- [9] J. G. Proakis, *Digital Communications*, 3rd ed. New York: McGraw-Hill, 1995.

²Turning off precoding is equivalent to using $\mathbf{a} = [1, 0, 0, \dots, 0]^T$ in (2). Assume that the receiver estimates the composite channel $\mathbf{h}^* \equiv \mathbf{h} \otimes \mathbf{a}$. The transmitter does not need to inform the receiver about its choice of the precoder. Thus, turning off precoding will not affect the receiver function.